A stress-activated neuronal ensemble in the supramammillary nucleus encodes anxiety but not memory

Jinming Zhang[1], Kexin Yu[1], Junmin Zhang[1], Yuan Chang[2], Xiao Sun[1], Zhaoqiang Qian[3], Zongpeng Sun[4], Zhiqiang Liu[1], Wei Ren[1,5], Jing Han[1,6,*]

1. Key Laboratory of Modern Teaching Technology, Ministry of Education, Shaanxi Normal University, Xi'an, 710062, China
2. Department of Histology and Embryology, School of Basic Medical Science, Xi'an Medical University, Xi'an, 710021, China
3. Laboratory Animal Center, Shaanxi Normal University, Xi'an, 710119, China
4. School of Psychology, Shaanxi Normal University, Xi'an, 710062, China
5. Faculty of Education, Shaanxi Normal University, Xi'an, 710062, China
6. Lead contact

*Correspondence:
Jing Han, Ph.D.
Key Laboratory of Modern Teaching Technology,
Ministry of Education,
Shaanxi Normal University,
9115 - 199 South Changan Road,
Xi'an, China, 710000
Tel/fax: +86-29-85308178
Email: jhan2012@snnu.edu.cn

Abstract

Anxiety is a prevalent negative emotional state induced by stress; however, the neural mechanism underlying anxiety is still largely unknown. We used acute and chronic stress to induce anxiety and test anxiety-like behavior; immunostaining, multichannel extracellular electrophysiological recording and Ca^{2+} imaging to evaluate neuronal activity; and virus-based neuronal tracing to label circuits and manipulate circuitry activity. Here, we identified a hypothalamic region, the supramammillary nucleus (SuM), as a key regulator of anxiety. We then characterized a small ensemble of stress-activated neurons (SANs) that are recruited in the encoding of anxiety. These SANs respond specifically to stress, and their activation robustly increases anxiety-like behavior in mice without significantly affecting fear memory. We also found that ventral subiculum (vSub)-SuM projections but not dorsal subiculum (dSub)-SuM projections encode anxiety and that inhibition of these vSub-SuM projections has an antianxiety effect. These results indicate that the reactivation of stress-activated supramammillary engram cells and relevant neural circuits are important neural processes underlying anxiety.

Keywords

Anxiety, Engram, Calcium activity, Supramammillary nucleus, Subiculum, Social stress

Introduction

Anxiety is a fundamental negative emotion observed in almost all mammal species. Long-lasting and uncontrollable anxiety often leads to several mental disorders, anxiety disorders, and even depression[1]. Recent studies have shown that the supramammillary nucleus (SuM), a part of the hypothalamus, regulates sleep[2], memory[3, 4], novelty exploration[3, 5], social memory[6, 7], neurogenesis[8], consciousness[9], locomotor activity[10], and theta oscillations in the hippocampus[11]. Projections from the SuM to the hippocampus have been largely studied and were found to modulate either episodic memory[3] or social memory[6, 7] in depending on the subregion of the hippocampus targeted. Although the SuM is located near the mammillary nucleus, a key region implicated in emotion regulation via the Papez circuit, its role in regulating emotion has been explored only superficially, without in-depth investigation. Despite some discussions of this role of the SuM, no consistent conclusion has been reached thus far[8, 12, 13].

Engram cells have been tagged and studied in many brain areas[14, 15]. Tagged engram cells react to specific stimuli, such as conditional stimuli[16, 17], pain[18], food[19], and even peripheral inflammation[20], and mediate the storage and retrieval of relevant memories. The manipulation of engrams can alleviate neurodegenerative diseases[21] or inflammation[20], suggesting the strong potential of engrams as therapeutic targets. Naturally, this has led us to consider whether there are special engram cells that encode anxiety. Despite the focus on the abovementioned topics, few studies have explored emotion-related engram cells[22]. Recent studies have focused on the role of the hippocampus and related neuronal afferents and efferents[23–25]. The dorsal part of the hippocampus mainly contributes to cognition, whereas the ventral hippocampus is often associated with emotion[26, 27]. Although the ventral hippocampus–hypothalamus circuit was reported to modulate anxiety[23, 24], it is still unknown whether the SuM is part of this regulatory circuit. Although the SuM sends and receives dense neuronal projections, few studies have focused on its afferents or its ability to modulate behavior and emotion[28].

In this study, we hypothesize that stress can recruit a special neuronal ensemble that exclusively encodes anxiety but not stress-induced fear memory. To test this hypothesis, we first used multiple methods to assess whether the SuM responds to acute or chronic stress. The activity of the SuM was chemogenetically manipulated, and anxiety-like behavior in rodents was tested. We subsequently employed the targeted recombination in active populations (TRAP) strategy to label and manipulate stress-activated neurons in the SuM to determine whether these cells function as engram cells. After demonstrating how the SuM modulates anxiety, we sought to identify upstream brain areas that may contribute to supramammillary function. We also examined the functions of neuronal projections from the ventral subiculum (vSub) to the SuM using fiber photometry to measure calcium dynamics, as well as chemogenetic manipulation. These results allowed us to characterize a previously unreported anxiety-specific engram cell ensemble in the SuM. In addition, we showed that projections from the vSub but not the dorsal subiculum (dSub) to the SuM govern chronic stress-induced anxiety-like behaviors.

Results

1. Stress increases neuronal activity in the SuM

c-Fos protein expression was assessed after acute stress exposure to test whether the SuM was activated (Figure 1 A). The number of c-Fos$^+$ cells was significantly increased by foot shock exposure (Figure 1 B-C). We next examined whether chronic stress affects neuronal activity in the SuM (Figure 1 D-E). We chose in vivo electrophysiological extracellular recordings to reveal the neuronal activity before and after chronic social defeat stress, the data shows that the firing rate of regular-spiking neurons (RNs) (Figure 1 F) but not fast-spiking neurons (FNs) (Supplemental Figure 1 A-B) increased after CSDS. Regarding local field potentials, there were no noticeable difference between the naïve and CSDS groups according to power spectrum analysis (Supplemental Figure 1 C-D). These results indicate that acute and chronic stress can strongly activate the supramammillary nucleus.

2. Activation of SuM produces anxiety-like behavior

After confirming the activation of SuM caused different types of stress, we then further investigate whether the SuM regulates anxiety behavior in mice. Chemogenetic manipulations were conducted to activate SuM neurons. The experiments were performed as shown in the workflow (Figure 2 A-B). The mice were subjected to the open field (OF) and EZM tests at least 2 weeks after virus injection, followed by a reward-seeking test (Figure 2 E-H, Supplemental Figure 2 A). CNO was administered intraperitoneally 30 minutes before the test. Chemogenetic activation of the SuM did not affect the performance of mice in the OF test (Figure 2 E-F, Supplemental Figure 2 B). Compared with control mice, mice in which the SuM was activated explored the open arms of the EZM less (Figure 2 G), despite no change in distance traveled (Supplemental Figure 2 C). Moreover, mice in which the SuM was activated consumed less food than control mice did (Figure 2 F). These data suggest that there are neuronal ensembles that control the expression of anxiety behavior.

3. Identification of stress-activated neurons in the SuM

We next investigated whether an ensemble that encodes stress and controls the expression of anxiety exists. By crossbreeding Fos 2A-iCreER(TRAP2) and Rosa26-LSL-tdTomato (Ai14) mice, we generated TRAP2;Ai14 mice in which engram cells were genetically tagged for visualization (Figure 3 A). Foot shock exposure strongly activated neurons in the SuM but not adjacent areas (Figure 3 B-C). We hypothesized that these stress-activated neurons (SANs) respond exclusively to stress, but not to other stimuli such as reward. To validate the activity-dependent labeling in TRAP2;Ai14 mice, we labeled SANs in two cohorts of mice exposed either to the home cage condition or to foot shock. Several days after labeling, the mice were exposed to either sucrose pellets or social stress to induce reward-related or stress-related c-Fos expression, respectively. The reactivation of SANs under reward stimulation and stress was then compared (Figure 3 D-H). Foot shocks dramatically activated and labeled neurons in the SuM (Figure 3 F). Social stress but not reward (presentation of sucrose pellets) induced neuronal activation (Figure 3 G) and led to a much greater chance of reactivation of SANs (Figure 3 H). These data suggest the specific regulatory effect of the SuM on the effects of stress but not reward and the potential existence of stress-encoding engram cells.

127 **4. Reactivation of SuM^{SANs} promotes anxiety-like behavior**

128 Foot shock exposure induces persistent context-dependent fear memory. To verify whether
129 tagged SANs in the SuM regulate fear memory, the mice were placed in Context B, which was
130 different from the context in which the foot shocks were presented. The freezing time was
131 calculated to assess the retrieval of fear memory (Supplemental Figure 3 A). CNO was given
132 30 minutes before the test, and mice in which Gq was activated did not exhibit a change in
133 freezing time (Supplemental Figure 3 B). When subjected to Context A, which was the same as
134 the context in which foot shocks were delivered, CNO-induced inactivation of SANs did not
135 alter the freezing time of the mice (Supplemental Figure 3 C), indicating that SANs in the SuM
136 did not encode memory.

137 To make sure foot shock induced anxiety won't last until manipulation, we subjected mice
138 to an acute stress protocol involving foot shocks and then performed the elevated plus maze
139 (EPM) and elevated zero maze (EZM) tests to evaluate anxiety on days 2 and 7 (Figure 4 A).
140 The mice that experienced foot shocks showed decreases in the exploration time in the open
141 arms on day 2. However, acute stress-induced anxiety was not detected on day 7 (Figure 4 B).
142 Seven days after SANs tagging, specific activation of SANs significantly increased the
143 concentration of corticosterone (a peripheral indicator of stress) in the mouse serum (Figure 4
144 C-D). Experiments involving chemogenetic manipulation also revealed the sound-selective
145 activation of SANs in the SuM (Figure 4 E-F). We then tested whether manipulating SANs in
146 the SuM influences the anxiety-like behavior of the mice. The mice were subjected to the OF
147 and EZM tests at least 1 week after SANs were tagged, followed by reward-seeking tests
148 (Figure 4 G-H). CNO was administered intraperitoneally 30 minutes before the test.
149 Chemogenetic activation of SANs decreased the total distance traveled by the mice in the OF
150 and EZM tests (Supplemental Figure 2 F-G). The mice also presented decreases in the distance
151 traveled in the central area (Figure 4 I) and time spent in the central area in the OF test (Figure
152 4 J), time spent in the open arms in the EZM test (Figure 4 K) and food consumption (Figure 4
153 L). These data suggest that SANs in the SuM encode anxiety but not fear memory.

154 **5. vSub-SuM projections encode anxiety-like behavior**

155 The SuM receives afferents from various brain areas, and we identified projections to the
156 SuM by using a nonvirus- and virus-based retrograde tracing strategy (Figure 5 A,
157 Supplemental Figure 4 A-C). Afferents from the dSub and vSub were identified using CTB-647
158 and AAV (Supplemental Figure 5 A-B). These projection neurons expressed Vglut1 RNA but
159 not Vgat RNA (Figure 5 B), suggesting that Sub-SuM projections are excitatory neuronal
160 projections, as Vglut1 is a crucial marker of glutamatergic neurons. We then performed an
161 electrophysiological experiment. Optogenetics-evoked postsynaptic currents in SuM neurons
162 were blocked by perfusion with DNQX, which indicates the existence of glutamatergic
163 projections from the Sub to the SuM (Figure 5 C-E). To investigate how Sub-SuM projections
164 modulate stress and anxiety-like behavior, we then used fiber photometry to measure the
165 calcium concentration to assess the activity patterns of the projection neurons (Figure 5 F-H).
166 The projection neurons in the vSub but not those in the dSub were more strongly activated
167 when the mice moved into the open arms from the closed arms of the EZM, (Figure 5 I-M).
168 Following exposure to acute stress, both dSub-SuM and vSub-SuM projection neurons

presented increased calcium activity (Figure 5 N-R). These data suggest that vSub-SuM projections, but not dSub-SuM projections, may participate in regulating anxiety.

6. Chronic inhibition of vSub-SuM projections alleviates anxiety-like behavior

After confirming the regulatory role of vSub-SuM projections in anxiety, we hypothesis that inhibition of this projection would alleviate chronic stress-induced anxiety. In the following experiments, the activity of these projections was chronically inhibited via a chemogenetic strategy. The mice were exposed to CSDS after the expression of the Gi protein was induced specifically on vSub-SuM projection neurons and their axons (Figure 6 A-B, D). The body weights of the mice were monitored throughout the entire procedure to assess their health (Figure 6 C). The mice showed no change in social interaction test scores after CSDS exposure (Figure 6 E). In the EZM test, the mice in which vSub-SuM projections were inhibited presented less anxiety-like behavior, as indicated by a longer time spent in the open arms of the EZM but no significant change in the distance traveled (Figure 6 F-G). Taken together, these data suggest that vSub-SuM projections are the essential neuronal projections for regulating anxiety.

Discussion

In this study, we combined multiple methods to determine that the SuM is the critical brain region that regulates anxiety. SuM neurons strongly respond to acute and chronic stress, and their activation results in robust increases in anxiety-like behavior in mice. We then defined a small ensemble of neurons that are activated by stress, called SANs. These SANs specifically respond to stressful stimuli but not reward. Selective activation of SANs in the SuM increases the serum concentration of corticosterone and anxiety-like behavior in mice. The neuronal circuits that may be underlie the regulation of anxiety were also determined in this study. The subiculum sends glutamatergic projections to the SuM and can be activated by stress, whereas only the vSub has a potential effect on the transition to anxiety. We finally determined that inhibition of SANs in the vSub project to the SuM is sufficient to alleviate anxiety in mice after CSDS exposure.

Regulation of anxiety by the SuM

The SuM has been demonstrated to respond to novel environments, social stimulation[3, 29], and stress[30, 31]. Given these findings, we assume that the SuM may be activated by foot shocks, a quantifiable acute stressor used in animal studies. Consistent with this hypothesis, we found that the SuM robustly positively responds to both acute and chronic stress through observable increases in c-Fos expression and the Ca^{2+} concentration in the neuronal body and increases in the neuronal firing rate. The activation of the SuM was also demonstrated to be essential for maintaining arousal[2, 9]. Sensitization to stressful events and high arousal are often associated with anxiety[32]. Thus, our data strongly suggest that the SuM potentially modulates anxiety. To further confirm whether the SuM participates in anxiety regulation, we recorded neuronal action potentials via multichannel extracellular recording while the mice were moving in the EPM, a traditional type of maze used to test anxiety in rodents. The change in the neuronal firing frequency when mice transitioned from the open arms to the closed arms supports the idea that the SuM may somewhat modulate anxiety. We then manipulated neuronal activity in the SuM via a chemogenetic method and subjected the mice to the EZM test, an

211 improved test for assessing anxiety in rodents. The decrease in the exploration time in the open
212 arms by mice in which the SuM was activated by hM3Dq indicated increased anxiety. We noted
213 that these results are inconsistent with those of some previous reports. Some studies have
214 reported that lesions in the SuM and adjacent areas decrease anxiogenic behavior in rats[11, 33,
215 34]. López-Ferreras et al. performed the OF test, a complicated test, and reported that the
216 chemogenetic activation of neurons in the SuM results in increased anxiety-like behaviors in
217 rats[12, 13]. However, further experiments involving specific test (e.g., the EZM test) are
218 needed to confirm whether there is a potential difference across species.

219 **Anxiety-related engram in the SuM**

220 Recent studies have highlighted the importance of activity-tagged neuronal ensembles in
221 regulating various behaviors, particularly memory[16, 35–37], food consumption[18], the
222 inflammatory response[20] and emotion[22, 38]. A negative experience-related neuronal
223 ensemble in the hippocampus was found to increase susceptibility to chronic stress[22]. A
224 recent study reported that the lateral habenula contains a small population of neurons that are
225 recruited in response to stress and mediate the development of depression in mice[38]. These
226 studies suggest that SANs may be critical for emotional regulation. In this study, we found that
227 the SuM was more strongly activated by acute stress than was adjacent areas. SANs were more
228 likely to be reactivated by social stress than by sucrose reward, indicating their potential to
229 specifically encode anxiety. As a classic marker of stress-induced anxiety in the peripheral
230 nervous system, the serum corticosterone concentration is usually used to estimate whether an
231 individual is anxious. Our data showed that the chemogenetic activation of SANs in the SuM
232 increased the serum corticosterone concentration, whereas the inactivation of SANs had no
233 effect. These findings in combination with the results of the OF, EZM, and contextual fear
234 memory tests suggest that SANs in the SuM store information about stress but not memory. We
235 also found that both the nonselective activation of SuM neurons and the selective activation of
236 SANs in the SuM significantly suppressed the consumption of sucrose pellets. This result may
237 be attributed to the anxiety-induced suppression of reward seeking[39]. However, further
238 experiments are still needed to confirm whether this effect is anxiety dependent and whether
239 basal food consumption is affected.

240 **A relevant neural circuit that regulates anxiety**

241 The SuM recruits and is targeted by neuronal projections in the hippocampus, medial
242 septum, and cortex[28]. To further understand the circuitry through which the SuM regulates
243 anxiety, we identified projections from the dSub and the vSub to the SuM[40]. Fiber photometry
244 was used to measure the Ca^{2+} concentration in projection neurons in the dSub and vSub, and
245 the results revealed increased Ca^{2+} activity in vSub-SuM projection neurons but not dSub-SuM
246 projection neurons when the mice transited from the closed arms to the open arms, indicating
247 that vSub-SuM projections encode anxiety. To confirm the regulation of anxiety by vSub-SuM
248 projections, we exposed mice to CSDS and found that constant inhibition of vSub-SuM activity
249 significantly abolished CSDS-induced anxiety in mice. Consistent with this result, selective
250 inhibition of $vSub^{SAN}$-SuM projections was also sufficient to alleviate anxiety. Unlike the dorsal
251 hippocampus, which is involved in the regulation of cognition, the ventral hippocampus is often
252 involved in regulating emotion[41]. The ventral CA1 area and its projections to the lateral

hypothalamic area were found to mediate innate anxiety, and its activation increases anxiety-like behavior in mice[24]. Although very close spatially, neurons in the subiculum are somewhat different from those in the CA1 region[42, 43]. The vSub and its downstream brain areas were found to regulate anxiety[44, 45]. Jing-Jing et al. reported that the vSub and its projections to the anterior hypothalamic nucleus are essential for anxiety because the inhibition of these projections decreases anxiety-like behavior[23]. Our data are consistent with these findings and suggest the mediating role of the vSub and its projections to different subareas in the hypothalamus.

In conclusion, the activation of SuM increases anxiety-like behavior. A neuronal ensemble activated by stress encodes anxiety but not memory. The activation of SANs also significantly increases anxiety-like behavior and suppresses reward seeking. SuM receives glutamatergic projections from the vSub, and inhibition of these projections can diminish CSDS-induced anxiety. These results suggest that stress may leave engram-like traces in the brain and that the activation of these engrams results in anxiety.

Acknowledgment

We thank Dr. Wenting Wang for his generous gift of the transgenic mice. We thank all the members of MTT for their valuable comments.

This research was funded by the National Natural Science Foundation of China (No. 82371518, No. 82071516), STI 2030—Major Projects 2021ZD0200500, the Humanities and Social Science Fund of the Ministry of Education of China (No. 22XJC880005), the Innovation Capability Support Program of Shaanxi (Program No. 2021PT-055), the Natural Science Basic Research Plan in Shaanxi Province of China (Program No. 2024JC-YBQN-0902), and the Scientific and Technological Innovation Team of Shaanxi Innovation Capability Support Plan (No. 2022TD-47).

Disclosures

The authors declare that they have no competing interests.

Methods and Materials

Animals

Male C57BL6/J mice aged 12–20 weeks were used. Fos$^{2A\text{-}iCreER}$ (TRAP2) mice were a gift from Wenting Wang (JAX, cat. No. 030323). Rosa26-CAG-LSL-tdTomato (Ai14) mice were purchased from the Shanghai Model Organisms Center (cat. No. NM-KI-225042). Male CD-1 mice aged 8–10 months were purchased from Charles River (cat. No. 201). To construct TRAP2;Ai14 mice, homozygous male TRAP2 mice and homozygous female Ai14 mice were bred. Homozygous TRAP2;Ai14 mice were maintained and used in the experiments. We performed genotyping for TRAP2 and Ai14 via PCR with the following primers: TRAP2 (wild-type: 357 bp, mutant: 232 bp): wild-type forward: GTCCGGTTCCTTCTATGCAG, mutant forward: CCTTGCAAAAGTATTACATCACG, common: GAACCTTCGAGGGAAGACG; Ai14 (wild-type: 297 bp, mutant: 196 bp): wild-type forward:

AAGGGAGCTGCAGTGGAGTA, wild-type reverse: CCGAAAATCTGTGGGAAGTC, mutant forward: GGCATTAAAGCAGCGTATCC, mutant reverse: CTGTTCCTGTACGGCATGG.

The mice were housed 4–5 per cage at a constant temperature and humidity (22 ± 1°C, 30–40% RH)on a day–night cycle (lights on from 08:00–20:00) with a fixed-intensity light source. Each mouse was acclimated to the testing environment for 1–2 min. Acclimation was performed for three days before the behavioral experiments. The mice were fed ad libitum and euthanized with CO_2 after all the tests were finished. The experimental protocols described here were approved by the Animal Ethics Committee of Shaanxi Normal University.

Behavioral procedure

Acute stress exposure

The mice were exposed to acute stress according to a previously reported procedure[46]; specifically, they were exposed to 20 foot shocks with an intensity of 0.5 mA that were randomly delivered across 10 minutes. The foot shocks were delivered in a fear conditioning box (Med-associates).

Chronic stress exposure

We used a CSDS protocol to induce anxiety and depression in the mice[47]. Each C57BL6/J mouse was housed with one CD-1 mouse, and the mice were separated by a transparent plexiglass board with several small holes. The mice were allowed to contact each other directly for 10 minutes every day for 10 days. Body weight was measured and recorded every day before contact.

OF test

The OF test was carried out in a 50 × 50 × 35 cm arena made of white plexiglass. The mice were allowed to move freely in the arena for 10 minutes, and the distance the mice traveled and the time the mice spent in the central area were recorded and analyzed.

EPM test

The EPM consisted of two open arms (30 × 7 cm), two closed arms (30 × 7 × 14 cm) and a central area (7 × 7 cm). The mice were allowed to move freely in the arena for 10 min, and the time the mice spent in the open arms was recorded and analyzed.

EZM test

The EZM was used to test whether the mice were anxious. The EZM used in this study was made of organic glass (height of 60 cm), with an inner diameter of 51.8 cm and an outer diameter of 65 cm. The closed arms of the EZM were separated by two 15 cm-high pieces of organic glass, the outer one of which was opaque. After a 15-minute habituation period, the mice were placed into the EZM and allowed to move freely for 10 minutes. Videos were recorded and analyzed using EthoVisionXT software. The time that the mice spent in the open arms was compared between the groups to evaluate anxiety-like behavior.

Reward seeking

On the first day, sucrose pellets were provided for habituation. The mice were then deprived of food on the second day. On the third day, the mice were placed in a new home cage without bedding and allowed to eat freely for 2 hours. The pellets were weighed to evaluate

335 whether the experimental manipulation influenced reward seeking by the mice.

336 **Social interaction test (SIT)**

337 The SIT was conducted as previously described[47]. The SIT involved two 2.5-minute
338 phases. In the first phase (no-target phase), we placed each C57BL6/J mouse in the periphery
339 of the arena opposite the social interaction area (SIA). We allowed the animal to explore the
340 arena freely. In the second phase (with-target phase), each C57BL6/J mouse was placed in the
341 arena again, with a new CD-1 mouse in the SIA. The social interaction ratio (SIR) was
342 calculated using the following formula:

343 $$Social\ interaction\ ratio\ (SIR) = \frac{Time\ in\ SIA^{With-target} - Time\ in\ SIA^{No-target}}{Time\ in\ SIA^{With-target} + Time\ in\ SIA^{No-target}}$$

344 **Contextual fear conditioning (CFC)**

345 Contextual fear memory was examined using the CFC test as previously described[48, 49].
346 The mice were allowed to habituate to the fear conditioning box (MED-VFC-USB-M, Med
347 Associates) for 10 minutes (day 1, Context A). The mice were allowed to explore the box freely
348 for 4 minutes at the beginning of the learning phase (the cumulative freezing time during this
349 phase was set as the baseline). Three foot-shocks (0.75 mA, 2 s) were subsequently delivered
350 4, 6.25, and 8.5 minutes after the beginning of the experiment. Ninety seconds after the last
351 foot shock, the mice were returned to their home cage. The mice were returned to Context A on
352 the fifth day to test the "loss of function" of the engram cells due to CNO injection 30 minutes
353 before testing. The mice were returned to Context B on the fifth day to test the "gain of function"
354 of the engram cells due to CNO injection 30 minutes before testing. Videos were recorded and
355 analyzed using VideoFreeze software, a commercial software provided by Med Associates.

356 **Neuronal tagging of stress-activated neurons**

357 To specifically label SANs, TRAP2 or TRAP2;Ai14 mice were intraperitoneally (i.p.)
358 injected with 4-hydroxytamoxifen (4-OHT, 50 mg/kg) immediately after acute stress exposure
359 or the learning phase of the CFC test. The mice were subjected to the next experiment or test
360 after 7 days to allow Cre-dependent recombination.

361 4-OHT (CAS No. 68392-35-8. Sigma, cat. No. H6278 or Bidepharm, cat. No.
362 BD00958757) was dissolved in DMSO at a concentration of 62.5 mg/mL and diluted with
363 vehicle (containing 10% TWEEN-80 and 80% saline) on the day of neuronal tagging. The final
364 concentration of DMSO was kept below 10% to avoid toxicity.

365 **Observation of the reactivation of SANs**

366 One week after neuronal tagging, whether previously tagged SANs were reactivated in
367 TRAP2;Ai14 mice when they were subjected to social stress was assessed. The mice in the first
368 group were underwent neuronal tagging in their home cages, and c-Fos expression was induced
369 by sucrose pellets. The mice in the second group were subjected to neuronal tagging in response
370 to foot shock exposure, and c-Fos expression was induced by sucrose pellets. The mice in the
371 third group were subjected to neuronal tagging in response to foot shock exposure, and c-Fos
372 expression was induced by social stress (one CD-1 mouse was placed in the home cage). The
373 mice were then sacrificed 90 minutes after sucrose pellet feeding or social stress exposure, and
374 c-Fos immunofluorescence staining was performed. The number of c-Fos-positive neurons was

375 counted to determine whether reward and cross-strain social stress could activate neurons in
376 the SuM. The likelihood of SAN reactivation was calculated using the following formula:

377 $$Reactivation\ chance\ (\%) = (c - Fos^{+}/DAPI^{+}) \times (tdTomato^{+}/DAPI^{+}) \times 100$$

378 **Viral vectors**

379 An adeno-associated virus (AAV) vector was used to label and manipulate specific neurons
380 or determine the calcium concentration. To manipulate the neuronal activity in the SuM,
381 AAV2/9-hSyn-hM3Dq-EGFP (titer: 5.00E+12 GC/mL, BrainVTA, cat. No. PT-0891) or its
382 control vector AAV2/9-hSyn-EGFP (titer: 5.00E+12 GC/mL, BrainVTA, cat. No. PT-1990) was
383 injected into the SuM of mice.

384 To manipulate the activity of SANs in the SuM, AAV2/9-hSyn-DIO-hM3Dq -EGFP (titer:
385 5.00E+12 GC/mL, BrainVTA, cat. No. PT-0891) or its control vector AAV2/9-hSyn-DIO-
386 EGFP (titer: 5.00E+12 GC/mL, BrainVTA, cat. No. PT-1103) was injected into the SuM of
387 TRAP2 mice.

388 To chronically inhibit vSub-SuM circuitry activity, AAV2/Retro-hSyn-Cre (titer:
389 2.00E+12 GC/mL, Taitool, cat. No. S0278) was injected into the SuM, and AAV2/9-hSyn-DIO-
390 hM4Di-mCherry (titer: 2.00E+12 GC/mL, Taitool, cat. No. S0193) or its control vector
391 AAV2/9-hSyn-DIO-mCherry (titer: 2.00E+12 GC/mL, Braincase, cat. No. BC-0025) was
392 injected into the vSub of wild-type mice.

393 To determine the calcium concentration in dSub/vSub-SuM projection neurons,
394 AAV2/Retro-hSyn-Cre (titer: 2.00E+12 GC/mL, Taitool, cat. No. S0278) was injected into the
395 SuM, and AAV2/9-hSyn-DIO-GCaMP7b (titer: 5.00E+12 GC/mL, BrainVTA, cat. No. PT-
396 2892) was injected into the dSub/vSub of wild-type mice.

397 For the ex vivo electrophysiological experiment, AAV2/9-hSyn-ChR2-mCherry (titer:
398 5.00E+12 GC/mL, BrainVTA, cat. No. PT-0150) was injected into the vSub of wild-type mice.

399 **Neuronal tracing**

400 Retrograde neuronal tracing was initially performed via injection of a serotype-2 AAV
401 vector (AAV2/Retro-hSyn-EGFP, titer: 5.00E+12 GC/mL, Taitool, cat. No. S0237) and CTB-
402 647 (1 μg/μL, Thermo Fisher, cat. No. C34778) into the SuM of wild-type mice. The mice were
403 then sacrificed after 2 weeks, and the brains were cut into coronal slices for imaging.

404 To precisely trace neuronal afferents projecting to SuM^{SANs}, AAV2/9-Ef1α-DIO-RVG
405 (titer: 5.00E+12 GC/mL, BrainVTA, cat. No. PT-0061) and AAV2/9-Ef1α-DIO-mCherry-F2A-
406 TVA (titer: 5.00E+12 GC/mL, BrainVTA, cat. No. PT-0207) were injected into the SuM of
407 TRAP2 mice simultaneously. The rabies virus (RV) vector RV-ENVA-ΔG-EGFP (titer:
408 2.00E+08 IFU/mL, BrainVTA, cat. No. R01001) was injected into the SuM 2 weeks after
409 neuronal tagging. The mice were then sacrificed after 2 weeks, and the brains were cut into
410 coronal slices for imaging.

411 **Stereotaxic surgery**

412 The mice were anesthetized using isoflurane at a concentration of 1.5~2.0%. Virus was
413 injected into the SuM (AP: -2.8, ML: 0, DV: -4.5 mm), dSub (AP: -2.8, ML: ±0.7, DV: -1.7
414 mm) or vSub (AP: -3.5, ML: ±3.0, DV: -4.6 mm) according to the experimental design. If only
415 one type of virus needed to be injected into a single brain area, the final volume was typically

150 nL. Otherwise, the final volume of the virus mixture was 200 nL. The viruses were injected at a rate of 50 nL/min. The syringe was held in place for at least 5 minutes and carefully removed from the brain. The mice were then returned to their home cages, and their health was monitored on the following days. All the mice that underwent surgery were subjected to the subsequent experiment after 2 weeks or more to allow virus expression.

For fiber photometry, ceramic ferrules (outer diameter: 2.5 mm, core diameter: 0.2 mm, NA: 0.50) were inserted into the dSub (AP: -2.8, ML: ±0.7, DV: -1.5 mm) or vSub (AP: -3.5, ML: ±3.0, DV: -4.4 mm) 2 weeks after virus injection under the guidance of a laser (wavelength: 470 nm). Calcium imaging was conducted at least 1 week after ferrule implementation.

Fiber photometry

Commercially available equipment (Thinker Tech) was used to determine the calcium concentration. The fluorescence signal was activated by a laser at 470 nm, and the signal was transmitted through a low-autofluorescence fiber–optic patch cord and rotary (doric lenses) and collected. The final activation intensity was set to ~40 μW. The sampling rate was 50 Hz for all the recordings. The mice were habituated to the fiber–optic patch cord for 3 consecutive days before recording. A TTL lasting 0.1 s was delivered by the software to mark the timepoint when the mouse moved from a closed arm to an open arms in the EPM (USB-IO box, Noldus). Continuous data were stored as *.tdms files and analyzed using custom-made software in MATLAB.

Chemogenetic manipulation

To manipulate neuronal activity in the SuM in wild-type and TRAP2 mice, clozapine N-oxide (CNO, 5 mg/kg; Cayman, cat. No. 25780) was injected i.p. 30 minutes before behavioral tests were performed. For chronic inhibition of circuit activity, CNO was administered orally (25 mg/L).

For acute and chronic experiments, CNO was dissolved in DMSO at a concentration of 10 mg/mL and stored at -20°C or in saline at a concentration of 1 mg/mL and stored at -80°C. The storage solution was diluted with saline to a concentration of 0.75 mg/mL to prepare a working solution for acute manipulation or to a concentration of 25 mg/L to prepare a working solution for chronic inhibition on the day of the experiment.

Immunofluorescence

The mice were anesthetized with 20% urethane and perfused with PBS or saline. The mouse brain was dissected and immersed in 4% paraformaldehyde (PFA) at 4°C overnight. The PFA solution was then replaced with a 30% sucrose solution. After the brain sank to the bottom, it was embedded in optimal cutting temperature (OCT) compound and frozen in a cryostat (CM1950, Leica). Coronal slices (40 μm) were cut and collected in a 24-well plate. After the residual OCT was removed with PBS, the slices were blocked with 0.3% Triton X-100 and 10% normal donkey serum at room temperature (RT) for 2 hours. The slices were then incubated with diluted primary antibody (rabbit anti-c-Fos, 1:500, Cell Signaling Technology, cat. No. 2250) at 4°C overnight. The next day, the slices were washed and incubated with secondary antibody dilutions (donkey anti-rabbit conjugated to AF647, 1:500, Jackson ImmunoResearch, cat. No. 706-605-148) at RT for 2 hours. After washing, the slices were transferred to slides and mounted with an antifade reagent (Thermo Fisher, cat. No. P36981). Images of the slices were

collected using a Zeiss M2 microscope and then analyzed.

RNA fluorescence in-situ hybridization

The samples were processed as described in the *Immunofluorescence* section. Slices (10 μm thick) were cut and dried at RT for ~15 minutes and then heated at 37°C for 30 minutes in a hybridization oven. The baked slides were then moved to precooled 4% PFA solution for fixation (~15 minutes). The slices were dehydrated in 100% ethanol at RT for 5 minutes. The dehydration step was then repeated. The following steps were performed as recommended by the manufacturer (ACDbio, cat. No. 323100). To label vglut1, vglut2 and vgat RNA, the slices were hybridized with Mm-*Slc17a7* (ACDbio, cat. No. 416631-C1), Mm-*Slc17a6* (ACDbio, cat. No. 319171-C1) and Mm-*Slc32a1* (ACDbio, cat. No. 319191-C3), respectively. The samples were then stained with Opal dye.

Costaining of protein and RNA

After confirming RNA staining, the slices were blocked in 10% normal goat serum for 1 hour. The blocking solution was removed, and the slices were incubated with diluted primary antibody (mouse anti-GFP, 1:500, Thermo Fisher, cat. No. MA5-16256; rabbit anti-tdTomato, 1:500, Oasis BioFarm, cat. No. OB-PRB013) at 4°C overnight. The slides were washed with PBS and incubated with secondary antibody solution (goat anti-rabbit/mouse conjugated to HRP, Proteintech, cat. No. PR30009) at RT for 1 hour (in the dark). After washing, the slices were stained with Opal dye at RT for 30 minutes. The slides were then mounted and imaged.

Corticosterone assay

Mouse whole blood was collected 90 min after CNO injection (5 mg/kg, i.p.). The samples were subsequently centrifuged at 2000×g for 10 minutes at 4°C after being left to stand at RT for 30–60 minutes. The supernatant was then carefully collected as the serum. Corticosterone levels were then measured using a commercial ELISA kit (Beyotime, cat. No. PC100) according to the manufacturer's instructions.

Ex vivo electrophysiology

The mice were anesthetized with urethane and then decapitated. The brain was quickly removed from the skull and immersed in precooled sucrose-based cutting solution (in mM, 225 sucrose, 2.5 KCl, 1.25 NaH_2PO_4, 26 $NaHCO_3$, 11 D-glucose, 5 L-ascorbic acid, 3 sodium pyruvate, 7 $MgSO_4 \cdot 7H_2O$, 0.5 $CaCl_2$). After being fixed on a metal pallet, the brain was cut into 300-μm slices. The slices were then collected and incubated in artificial cerebrospinal fluid (ACSF) containing (in mM) 122 NaCl, 2.5 KCl, 1.25 NaH_2PO_4, 26 $NaHCO_3$, 11 D-glucose, 2 $MgSO_4 \cdot 7H_2O$, and 2 $CaCl_2$ equilibrated with 95% O_2-5% CO_2 at 28°C for at least 1 hour before recording.

To evoke postsynaptic currents (PSCs) using light, whole-cell recording of neurons near axons illuminated by ChR2-mCherry injected into the vSub was performed. The final light intensity at the end of the optical fiber was set to ~5 mW/mm^2. Then, blue light (470 nm, width: 10 ms, frequency: 0.05 Hz) was used to evoke optically induced PSCs (oPSCs). DNQX (20 μM) was perfused into the ACSF to isolate AMPA-dependent currents from the oPSCs after establishing a 5-minute baseline.

In vivo electrophysiology

The mice were anesthetized with 2% isoflurane and fixed to a stereotaxic device. A sixteen-channel microwire electrode array (KD-MWA, KedouBC), a 4x4 array of 25 μm NiTi wires spaced 200 μm apart, was slowly inserted into the mouse brain. Four small nails were first inserted into the skull, with a ground wire presoldered onto one of them. The electrode array was left in the SuM (AP: -2.8, ML: 0, DV: -4.55 mm), and then dental cement was used to fix it onto the skull.

The mice were introduced to the recording area at least one week after surgery. During the day, the electrode array attached to the mouse skull was connected to the OpenEphys acquisition board through an Intan head stage. An OpenEphys GUI was used to visualize and save electrical signals. The mice were allowed to move freely inside a home cage-like arena for at least 20 minutes. Only data acquired during the last 5 min were saved and then analyzed via Python-based software and a customized Python script.

Spikes were detected and divided into single units using SpikeInterface (https://github.com/SpikeInterface/spikeinterface). Continuous binary raw data (sampling rate: 30 kHz) were imported and filtered using a bandpass butter filter at a cutoff value of 300 Hz. Movement artifacts were removed by subtracting medians across all channels. The templates were then extracted and fitted using spyking-circus2 inside the SpikeInterface frame. Neurons meeting the following criteria were excluded from the subsequent analysis: (1) spikes with refracting period violations smaller than 1 ms, accounting for more than 2% of total spikes, and (2) a total frequency lower than 0.2 Hz. Neurons with spike frequencies ≥ 10 Hz were considered RNs, whereas those with spike frequencies < 10 Hz were considered FNs, as reported in a previous study[3]. The local field potential was extracted and analyzed using the power spectrum analysis tool in MATLAB.

Statistical analysis

The data are presented as the means ± SEMs in all the figures in this manuscript. For normally distributed data with equal standard deviations, independent t tests for unpaired data and dependent t tests for paired data were performed in GraphPad software to compare mean values between two groups. Otherwise, the Mann–Whitney test for unpaired data and the Wilcoxon test for paired data were performed instead. One-way ANOVA followed by Tukey's post hoc test and two-way ANOVA followed by Sidak's post hoc test were performed to compare mean values among more than three groups. A p value less than 0.05 was considered to indicate a statistically significant difference between groups. "*" represents $p < 0.05$, "**" represents $p < 0.01$, and "***" represents $p < 0.001$.

538 **References**

539

540 1. Nettle D, Bateson M. The evolutionary origins of mood and its disorders. Current
541 Biology. 2012;22.

542 2. Liang M, Jian T, Tao J, Wang X, Wang R, Jin W, et al. Hypothalamic supramammillary
543 neurons that project to the medial septum modulate wakefulness in mice. Commun
544 Biol. 2023;6.

545 3. Chen S, He L, Huang AJY, Boehringer R, Robert V, Wintzer ME, et al. A
546 hypothalamic novelty signal modulates hippocampal memory. Nature. 2020;586:270–
547 274.

548 4. Li Y, Bao H, Luo Y, Yoan C, Sullivan HA, Quintanilla L, et al. Supramammillary
549 nucleus synchronizes with dentate gyrus to regulate spatial memory retrieval through
550 glutamate release. Elife. 2020;9.

551 5. Kesner AJ, Shin R, Calva CB, Don RF, Junn S, Potter CT, et al. Supramammillary
552 neurons projecting to the septum regulate dopamine and motivation for environmental
553 interaction in mice. Nat Commun. 2021;12.

554 6. Qin H, Fu L, Jian T, Jin W, Liang M, Li J, et al. REM sleep-active hypothalamic
555 neurons may contribute to hippocampal social-memory consolidation. Neuron.
556 2022:1–15.

557 7. Li J, Sun X, You Y, Li Q, Wei C, Zhao L, et al. Auts2 deletion involves in DG
558 hypoplasia and social recognition deficit: The developmental and neural circuit
559 mechanisms. Sci Adv. 2022;8:1238.

560 8. Li YD, Luo YJ, Chen ZK, Quintanilla L, Cherasse Y, Zhang L, et al. Hypothalamic
561 modulation of adult hippocampal neurogenesis in mice confers activity-dependent
562 regulation of memory and anxiety-like behavior. Nat Neurosci. 2022;25:630–645.

563 9. Pedersen NP, Ferrari L, Venner A, Wang JL, Abbott SBG, Vujovic N, et al.
564 Supramammillary glutamate neurons are a key node of the arousal system. Nat
565 Commun. 2017;8.

566 10. Farrell JS, Lovett-Barron M, Klein PM, Sparks FT, Gschwind T, Ortiz AL, et al.
567 Supramammillary regulation of locomotion and hippocampal activity. Science (1979).
568 2021;374:1492–1496.

569 11. Pan WX, McNaughton N. The role of the medial supramammillary nucleus in the
570 control of hippocampal theta activity and behaviour in rats. European Journal of

571 Neuroscience. 2002;16:1797–1809.

572 12. López-Ferreras L, Eerola K, Shevchouk OT, Richard JE, Nilsson FH, Jansson LE, et
573 al. The supramammillary nucleus controls anxiety-like behavior; key role of GLP-1R.
574 Psychoneuroendocrinology. 2020;119.

575 13. López-Ferreras L, Eerola K, Mishra D, Shevchouk OT, Richard JE, Nilsson FH, et al.
576 GLP-1 modulates the supramammillary nucleus-lateral hypothalamic neurocircuit to
577 control ingestive and motivated behavior in a sex divergent manner. Mol Metab.
578 2019;20:178–193.

579 14. Tonegawa S, Liu X, Ramirez S, Redondo R. Memory Engram Cells Have Come of
580 Age. Neuron. 2015;87:918–931.

581 15. Josselyn SA, Tonegawa S. Memory engrams: Recalling the past and imagining the
582 future. Science (1979). 2020;367.

583 16. Liu X, Ramirez S, Pang PT, Puryear CB, Govindarajan A, Deisseroth K, et al.
584 Optogenetic stimulation of a hippocampal engram activates fear memory recall.
585 Nature. 2012;484:381–385.

586 17. Guenthner CJ, Miyamichi K, Yang HH, Heller HC, Luo L. Permanent genetic access
587 to transiently active neurons via TRAP: Targeted recombination in active populations.
588 Neuron. 2013;78:773–784.

589 18. Sun H, Li Z, Qiu Z, Shen Y, Guo Q, Hu SW, et al. A common neuronal ensemble in
590 nucleus accumbens regulates pain-like behaviour and sleep. Nat Commun. 2023;14.

591 19. Azevedo EP, Pomeranz L, Cheng J, Schneeberger M, Vaughan R, Stern SA, et al. A
592 Role of Drd2 Hippocampal Neurons in Context-Dependent Food Intake. Neuron.
593 2019;102:873-886.e5.

594 20. Koren T, Yifa R, Amer M, Krot M, Boshnak N, Ben-Shaanan TL, et al. Insular cortex
595 neurons encode and retrieve specific immune responses. Cell. 2021;184:5902-
596 5915.e17.

597 21. Ryan TJ, Roy DS, Pignatelli M, Arons A, Tonegawa S. Engram Cells Retain Memory
598 Under Retrograde Amnesia. Science (1979). 2015;348:1007–1013.

599 22. Zhang TR, Larosa A, Di Raddo ME, Wong V, Wong AS, Wong TP. Negative memory
600 engrams in the hippocampus enhance the susceptibility to chronic social defeat stress.
601 Journal of Neuroscience. 2019;39:7576–7590.

602 23. Yan JJ, Ding XJ, He T, Chen AX, Zhang W, Yu ZX, et al. A circuit from the ventral

603 subiculum to anterior hypothalamic nucleus GABAergic neurons essential for anxiety-
604 like behavioral avoidance. Nat Commun. 2022;13.

605 24. Jimenez JC, Su K, Goldberg AR, Luna VM, Biane JS, Ordek G, et al. Anxiety Cells in
606 a Hippocampal-Hypothalamic Circuit. Neuron. 2018;97:670-683.e6.

607 25. Forro T, Volitaki E, Malagon-Vina H, Klausberger T, Nevian T, Ciocchi S. Anxiety-
608 related activity of ventral hippocampal interneurons. Prog Neurobiol. 2022;219.

609 26. Strange BA, Witter MP, Lein ES, Moser EI. Functional organization of the
610 hippocampal longitudinal axis. Nat Rev Neurosci. 2014;15:655–669.

611 27. Fanselow MS, Dong HW. Are the Dorsal and Ventral Hippocampus Functionally
612 Distinct Structures? Neuron. 2010;65:7–19.

613 28. Kesner AJ, Mozaffarilegha M, Rajamani KT, Arima Y, Harony-Nicolas H,
614 Hashimotodani Y, et al. Hypothalamic Supramammillary Control of Cognition and
615 Motivation. Journal of Neuroscience, vol. 43, Society for Neuroscience; 2023. p.
616 7538–7546.

617 29. Cumbers MR, Chung ST, Wakerley JB. A neuromodulatory role for oxytocin within
618 the supramammillary nucleus. Neuropeptides. 2007;41:217–226.

619 30. Cristina M, Silveira L, Sandner G, Graeff FG. Induction of Fos immunoreactivity in
620 the brain by exposure to the elevated plus-maze. Behavioural Brain Research.
621 1993;56:115–118.

622 31. Escobedo A, Holloway SA, Votoupal M, Cone AL, Skelton H, Legaria AA, et al.
623 Glutamatergic supramammillary nucleus neurons respond to threatening stressors and
624 promote active coping. Elife. 2023;12.

625 32. Leduke DO, Borio M, Miranda R, Tye KM. Anxiety and depression: A top-down,
626 bottom-up model of circuit function. Ann N Y Acad Sci. 2023;1525:70–87.

627 33. Aranda L, Santín LJ, Begega A, Aguirre JA, Arias JL. Supramammillary and adjacent
628 nuclei lesions impair spatial working memory and induce anxiolitic-like behavior.
629 Behavioural Brain Research. 2006;167:156–164.

630 34. Beck' CHM, Fibiger HC. Conditioned Fear-induced Changes in Behavior and in the
631 Expression of the Immediate Early Gene c-fos: With and Without Diazepam
632 Pretreatment. The Journal of Neuroscience. 1995;15:709–720.

633 35. Tonegawa S, Morrissey MD, Kitamura T. The role of engram cells in the systems
634 consolidation of memory. Nat Rev Neurosci. 2018;19:485–498.

635 36. Sun X, Bernstein MJ, Meng M, Rao S, Sørensen AT, Yao L, et al. Functionally Distinct
636 Neuronal Ensembles within the Memory Engram. Cell. 2020;181:410-423.e17.

637 37. Lacagnina AF, Brockway ET, Crovetti CR, Shue F, McCarty MJ, Sattler KP, et al.
638 Distinct hippocampal engrams control extinction and relapse of fear memory. Nat
639 Neurosci. 2019;22:753–761.

640 38. Zheng Z, Liu Y, Mu R, Guo X, Feng Y, Guo C, et al. A small population of stress-
641 responsive neurons in the hypothalamus-habenula circuit mediates development of
642 depression-like behavior in mice. Neuron. 2024. 2024.
643 https://doi.org/10.1016/j.neuron.2024.09.012.

644 39. Peng B, Xu Q, Liu J, Guo S, Borgland SL, Liu S. Corticosterone attenuates reward-
645 seeking behavior and increases anxiety via D2 receptor signaling in ventral tegmental
646 area dopamine neurons. Journal of Neuroscience. 2021;41:1566–1581.

647 40. Tang H, Wu GS, Xie J, He X, Deng K, Wang H, et al. Brain-wide map of projections
648 from mice ventral subiculum. Neurosci Lett. 2016;629:171–179.

649 41. Shi HJ, Wang S, Wang XP, Zhang RX, Zhu LJ. Hippocampus: Molecular, Cellular, and
650 Circuit Features in Anxiety. Neurosci Bull. 2023;39:1009–1026.

651 42. Aggleton JP, Christiansen K. The subiculum: The heart of the extended hippocampal
652 system. Prog Brain Res. 2015;219:65–82.

653 43. Ding SL, Yao Z, Hirokawa KE, Nguyen TN, Graybuck LT, Fong O, et al. Distinct
654 Transcriptomic Cell Types and Neural Circuits of the Subiculum and Prosubiculum
655 along the Dorsal-Ventral Axis. Cell Rep. 2020;31.

656 44. Mueller NK, Dolgas CM, Herman JP. Stressor-selective role of the ventral subiculum
657 in regulation of neuroendocrine stress responses. Endocrinology. 2004;145:3763–
658 3768.

659 45. Ghasemi M, Navidhamidi M, Rezaei F, Azizikia A, Mehranfard N. Anxiety and
660 hippocampal neuronal activity: Relationship and potential mechanisms. Cogn Affect
661 Behav Neurosci. 2022;22:431–449.

662 46. Marcus DJ, Bedse G, Gaulden AD, Ryan JD, Kondev V, Winters ND, et al.
663 Endocannabinoid Signaling Collapse Mediates Stress-Induced Amygdalo-Cortical
664 Strengthening. Neuron. 2020;105:1062-1076.e6.

665 47. Kim H-D, Call T, Carotenuto S, Johnson R, Ferguson D. Testing Depression in Mice: a
666 Chronic Social Defeat Stress Model. Bio Protoc. 2017;7.

667 48. Zhang J, Zhang J, Yuan R, Han W, Chang Y, Kong L, et al. Inhibition of cannabinoid
668 degradation enhances hippocampal contextual fear memory and exhibits anxiolytic
669 effects. IScience. 2024;27:108919.

670 49. Chang Y, Zhang J, Zhang J, Zhu W, Zheng Q, Qian Z, et al. N6-methyladenosine RNA
671 modification of glutamatergic neurons is associated with contextual fear
672 discrimination. Physiol Behav. 2022;248:113741.

673

674

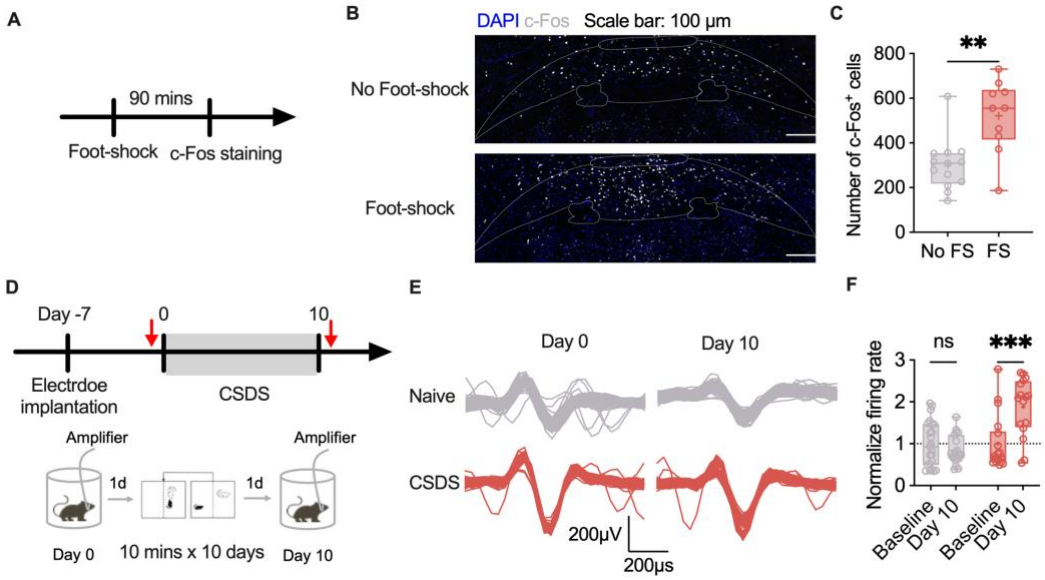

Figure 1. Stress activates the SuM

(A) Workflow of the c-Fos staining. **(B)** Representative images of c-Fos staining (DAPI: blue; c-Fos: white; scale bar: 100 μm). **(C)** Statistical analysis of the number of c-Fos-positive cells displayed in panel B. n = 10–13 per group; unpaired t test. **(D)** Workflow of CSDS exposure and in vivo recording. **(E)** Representative spikes acquired by multichannel recording. **(F)** Statistical analysis of the firing rates of RNs at baseline and after CSDS exposure. n = 16–23 per group; two-way ANOVA followed by Sidak's post hoc test. The data in C and F are presented as the means ± SEMs. "**", p <0.01; "***", p < 0.001. CSDS: chronic social stress; FS: foot shock. Also see **Supplemental Figure 1.**

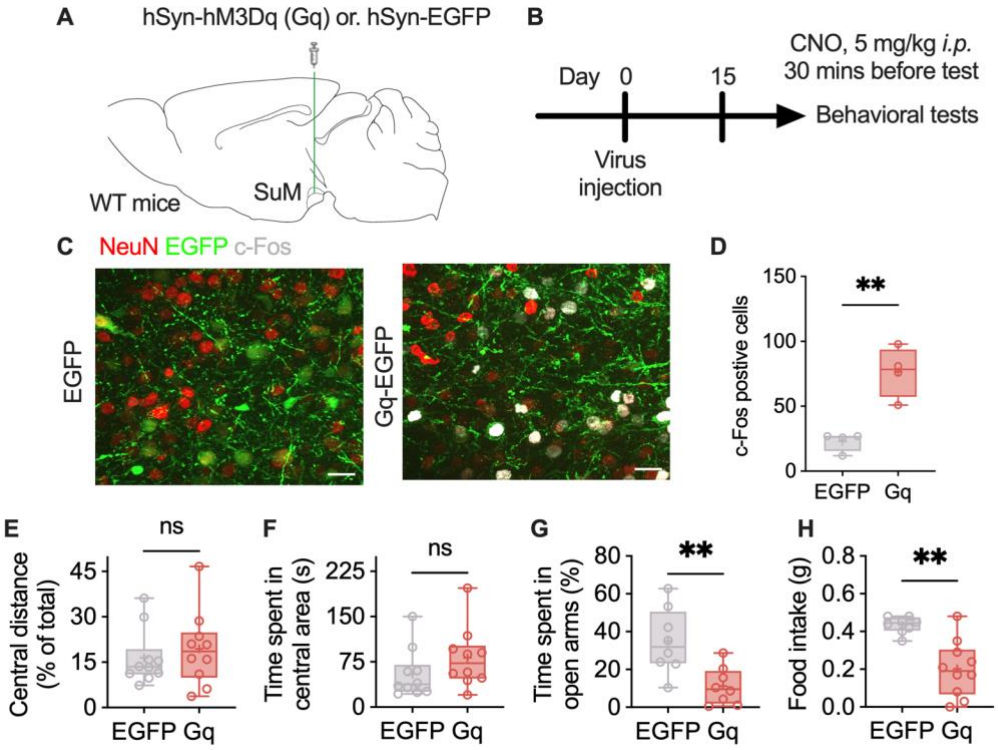

Figure 2. Activation of SuM produces anxiety-like behavior

(A-B) Virus injection information (A) and workflow for chemogenetic manipulation (B). **(C)** Representative c-Fos images. **(D)** Statistical analysis of the number of c-Fos-positive cells displayed in panel C. n = 4 per group; unpaired t test. **(E-F)** Statistical analysis of the distance traveled in the central area (E) and the time that the mice spent in the central area (F) in the OF test. n = 10 per group; unpaired t test for the data in (E) and the Mann–Whitney test for the data in (F). **(G)** Statistical analysis of the time that the mice spent in the open arms of the EZM. n = 8 per group; unpaired t test. **(H)** Statistical analysis of sucrose pellets consumed. n = 8–10 per group; Mann–Whitney test. The data in D-H are presented as the means ± SEMs. "ns", p >0.05; "**", p <0.01. Also see **Supplemental Figure 2.**

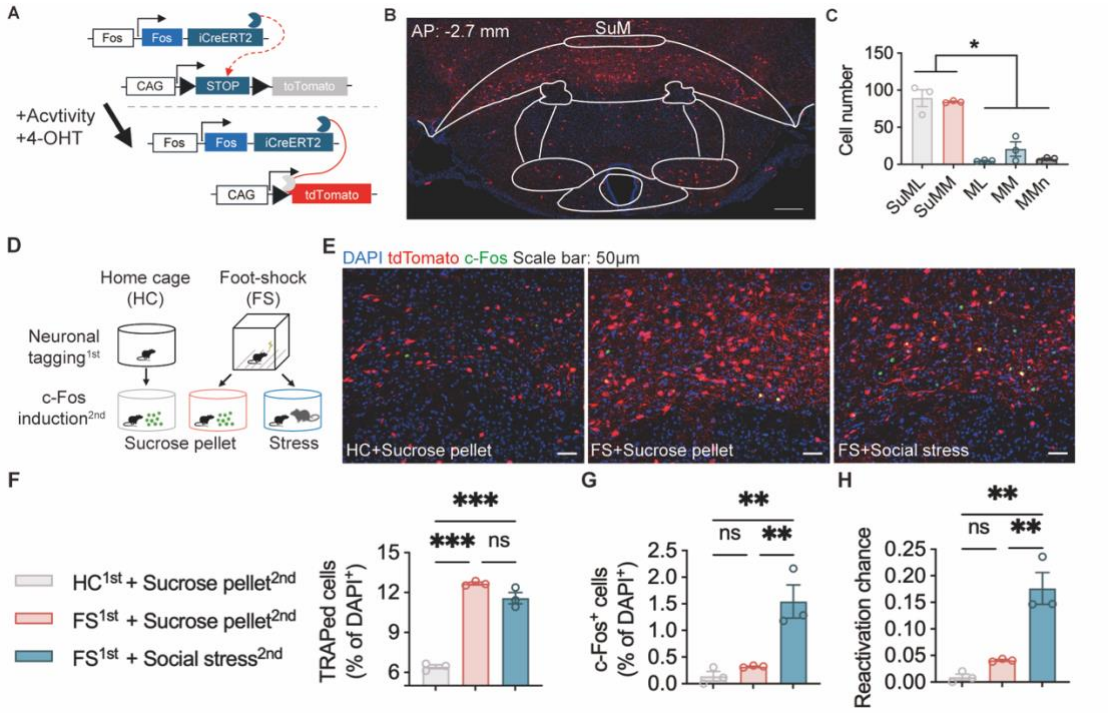

Figure 3. SANs in the SuM selectively respond to social stress but not reward

(A) Workflow of neuronal tagging. **(B)** Representative image of SANs in the SuM (DAPI: blue, tagged cells: red). **(C)** Quantitative statistics of stress-tagged cells in several brain areas. n = 3 per area; one-way ANOVA followed by Tukey'4s post hoc test. **(D)** Workflow of neuronal tagging and c-Fos staining. **(E)** Representative images of stress-tagged cells and c-Fos expression induced by sucrose and social stress (DAPI: blue, tdTomato: red, c-Fos: green). **(F)** Statistical analysis of the number of stress-tagged cells in the SuM. n = 3 per group; one-way ANOVA followed by Tukey's post hoc test. **(G)** Statistical analysis of the number of c-Fos^{+} cells after sucrose or social stress exposure. n = 3 per group; one-way ANOVA followed by Tukey's post hoc test. **(H)** Statistical analysis of the likelihood of reactivation of stress-tagged cells. n = 3 per group; one-way ANOVA followed by Tukey's post hoc test. The data in C and F-H are presented as the means ± SEMs. "ns", p >0.05; "*", p <0.05; "**", p <0.01; "***", p < 0.001.

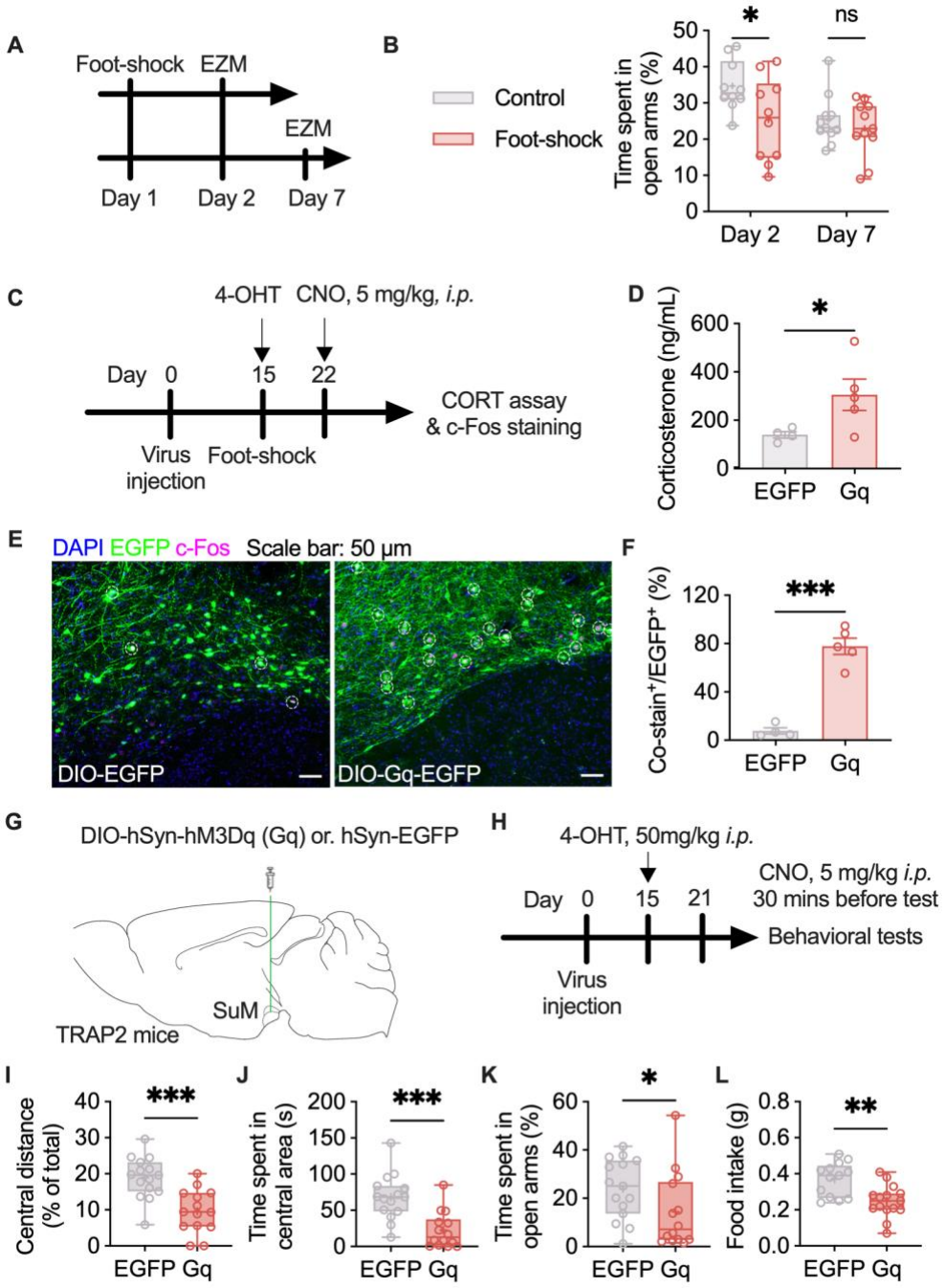

Figure 4. Selective chemogenetic activation of SANs elevates corticosterone level and produces anxiety-like behavior

(A) Workflow of the acute stress and anxiety tests. **(B)** Statistical analysis of the time that the mice spent in the open arms of the EZM. n = 10–11 per group; two-way ANOVA followed by Sidak post hoc test. **(C)** Workflow of the CORT assay and c-Fos staining. **(D)** Statistical analysis of the serum concentration of corticosterone after the application of CNO. n = 4-5 per group; unpaired t test. **(E)** Representative images of stress-tagged cells and c-Fos expression induced by chemogenetic manipulation (DAPI: blue, EGFP: green, c-Fos: violet). **(F)** Statistical analysis of the percentage of costained cells relative to EGPF$^+$ cells in the SuM. n = 4-5 per group; unpaired t test. **(G-H)** Virus injection information and workflow of

720 chemogenetic manipulation. **(I-J)** Statistical analysis of the distance traveled in the central area (I) and
721 the time that the mice spent in the central area (J) in the OF test. n = 14–15 per group; unpaired t test. **(K)**
722 Statistical analysis of the time that the mice spent in the open arms of the EZM. n = 14–15 per group;
723 Mann–Whitney test. **(L)** Statistical analysis of sucrose pellets consumed. n = 13–15 per group; unpaired
724 t test. The data in B, D, E and I-L are presented as the means ± SEMs. "*", $p < 0.05$; "**", $p < 0.01$; "***", p
725 < 0.001. Also see **Supplemental Figure 2.**
726

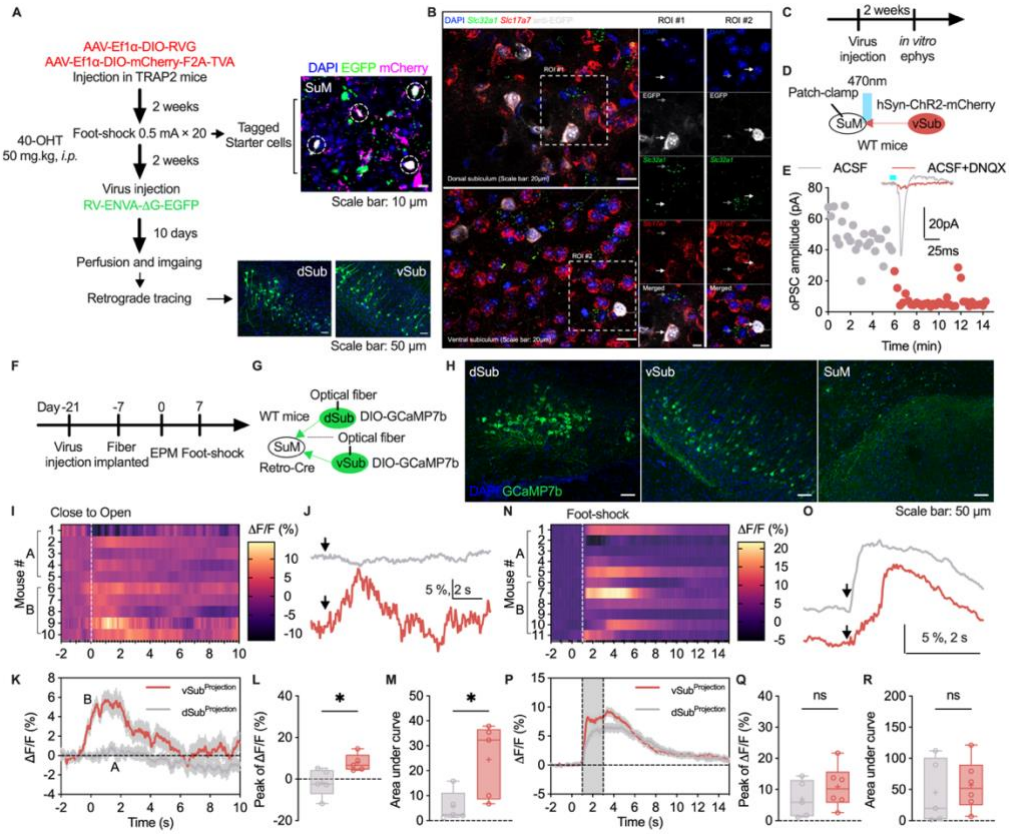

Figure 5. vSub-SuM projections encoding anxiety-like behavior

(A) Workflow of virus-based retrograde neuronal tracing. **(B)** Representative images of in situ RNA staining (DAPI: blue, Slc32a1: green, Slc17a7: red, EGFP: white). **(C)** Workflow of ex vivo electrophysiological recording. **(D)** Schematic of oPSCs in the SuM. **(E)** Representative traces of oPSCs. **(F)** Workflow of Ca^{2+} imaging. **(G)** Schematic of Ca^{2+} imaging of dSub and vSub projection neurons. **(H)** Representative images of GCaMP7b expression in the dSub, vSub and SuM (DAPI: blue, GCaMP7b: green). **(I)** Heatmap of the Ca^{2+} fluorescence intensity during the transition from the closed to the open arms. **(J)** Representative Ca^{2+} activity during the transition from the closed arms to the open arms. **(K)** Average ΔF/F of Ca^{2+} recorded in the dSub and vSub. **(L)** Statistical analysis of the peak Ca^{2+} activity. n = 5 per group; unpaired t test. **(M)** Statistical analysis of the area under the curve of Ca^{2+} activity. n = 5 per group; unpaired t test. **(N)** Heatmap of the Ca^{2+} fluorescence intensity during exposure to foot shocks. **(O)** Representative Ca^{2+} activity during exposure to foot shocks. **(P)** Average ΔF/F of Ca^{2+} recorded in the dSub and vSub. **(Q)** Statistical analysis of the peak Ca^{2+} activity. n = 5–6 per group; unpaired t test. **(R)** Statistical analysis of the area under the curve of Ca^{2+} activity. n = 5–6 per group; unpaired t test. Data in L-M and Q-R are presented as the mean ± SEM. "ns", p >0.05; "*", p <0.05. Also see **Supplemental Figure 4** & **Supplemental Figure 5.**

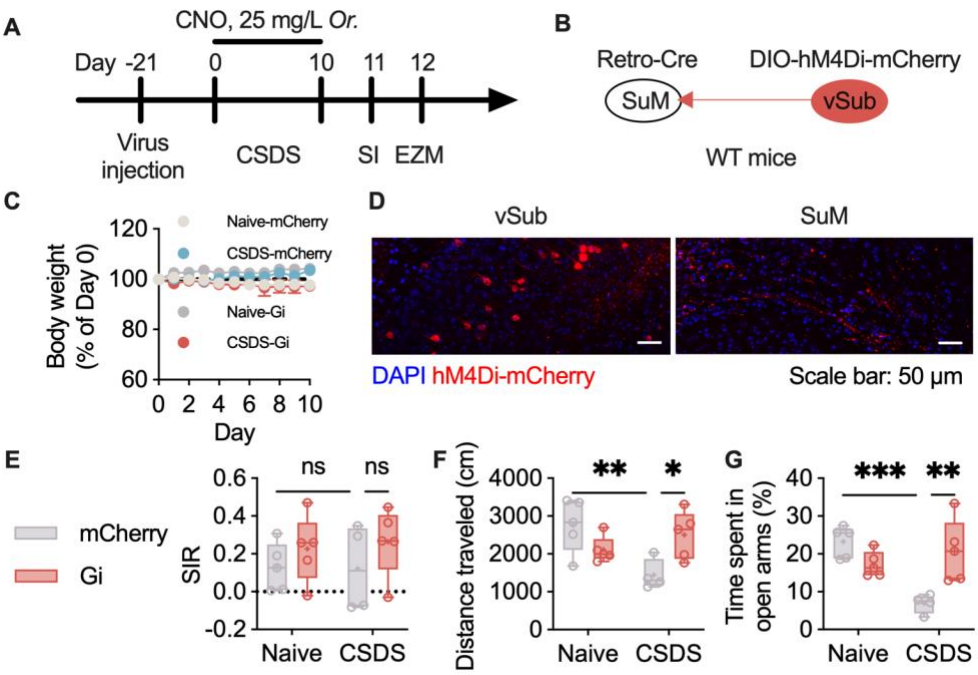

Figure 6. Selective inhibition of vSub-SuM projections alleviated CSDS-induced anxiety **(A)** Workflow of CSDS and chemogenetic manipulation. **(B)** Schematic of chemogenetic manipulation of specific projections. **(C)** Body weight during CSDS exposure. **(D)** Representative images of virus expression. **(E)** Statistical analysis of the social interaction ratio after CSDS exposure. n = 4–5 per group; two-way ANOVA followed by Sidak's post hoc test. **(F)** Statistical analysis of the distance that the mice traveled in the EZM. n = 4–5 per group; two-way ANOVA followed by Sidak's post hoc test. **(G)** Statistical analysis of the time that the mice spent in the open arms of the EZM; two-way ANOVA followed by Sidak post hoc test. The data in C and E-Gare presented as the means ± SEMs. "ns", p >0.05; "*", p <0.05; "**", p <0.01; "***", p < 0.001.